

2 μm emission from Si/Ge heterojunction LED and up to 1.55 μm detection by GOI detectors with strain-enhanced features

M. H. Liao^a, C.-Y. Yu^a, C.-F. Huang^a, C.-H. Lin^a, C.-J. Lee^a, M.-H. Yu^a, S. T. Chang^b, C.-Y. Liang^a, C.-Y. Lee^a, T.-H. Guo^a, C.-C. Chang^a, and C. W. Liu^{a*}

^aDepartment of Electrical Engineering, Graduate Institute of Electronics Engineering, and Graduate Institute of Electro-Optical Engineering, National Taiwan University, Taipei, Taiwan, R. O. C.

^bDepartment of Electrical Engineering, National Chung Hsing University, Taichung, Taiwan, R. O. C.

*E-mail: chee@cc.ee.ntu.edu.tw

Abstract

The Ge/Si heterojunction MOS LED can emit $\sim 2 \mu\text{m}$ light due to the radiative recombination at type II heterojunction. The fully depleted 800 nm germanium on insulator (GOI) can increase the responsivity and the speed of the MOS detector due to the large absorption of Ge and the electrical field in the active layer, respectively. Moreover, the external strain can tune the emission energy ($\sim 11 \text{ meV}$) by modifying the band structure. The responsivity of GOI MOS detector is also improved by $\sim 10\%$ using the external strain. Both heterojunction and strain (internal or external) can enhance the performance of Si-based optoelectronics.

Introduction

Due to the compatibility with Si technology, the Si-based optoelectronic devices are the holy grails for the full integration of electrical and optical devices. The band edge light emission of $\sim 1.1 \mu\text{m}$ wavelength from the Si MOS LED [1] and the high efficient Ge quantum dot MOS photodetector [2] were reported in the past. The electroluminescence (EL) of MIS structure is an effective indicator of Dit at the interface and the strain level in the Si channel by its intensity and energy position, respectively [3-4] for the future in-line inspection tool. In this paper, the mid-infrared emission of 2 to 2.4 μm is observed from Si/Ge heterojunction MOS LED for the first time and can be used for the detection of the explosives. To increase the responsivity of Si-based detectors, the thick Ge to increase the absorption is necessary. The thick epi-Ge on Si leads to high defect density, which significantly traps the photo-generated carriers. The bulk Ge has less defect density and can be transferred to Si or SOI substrates by smart cut and wafer bonding. The resulting GOI photodetector has the high responsivity and speed. Besides the mobility enhancement by strain [5], the optical absorption can be also enhanced by the strain to increase the detector responsivity. The strain, heterojunction, and Ge layer transfer can boost the optoelectronic performance of Si devices.

Fabrication and Characterization

The Ge quantum well ($\sim 4 \text{ nm}$) for light emitting diode

was directly grown on Si (100) at 525 $^{\circ}\text{C}$ by ultra-high-vacuum chemical vapor deposition (UHV/CVD). A passivated Si layer ($\sim 1 \text{ nm}$) was capped on epi-Ge layer to improve the interface between oxide and epi-Ge layer (Fig. 1(a)). The 2 nm oxide used for the tunneling oxide was grown by liquid phase deposition (LPD) at 60 $^{\circ}\text{C}$ to allow the carrier tunneling between the electrode and the semiconductor. Before oxidation, the sample was cleaned by a HF dip. The Al or Pt circular gate electrodes with various areas are defined by the shadow mask. Fig. 1(b) shows Raman spectra excited by the 514 nm Ar laser for the Ge quantum well on Si (curve 1) and bulk Si (curve 2). Since the bulk Si has the signal of $\sim 300 \text{ cm}^{-1}$ close to Ge signal, the Raman spectrum of the pure Ge layer on Si is obtained from the subtraction of the bulk Si signal from the measured spectrum of the Ge quantum well on Si. Note that the signal of thin Si cap (1 nm) is too weak to be measured. The resulting Raman spectrum of pure epi Ge without Si substrate interference has a broad feature located at $\sim 304.1 \text{ cm}^{-1}$ (curve 3 in Fig. 1(b)). As compared with the bulk Ge (curve 4), the Raman shift of Ge-Ge phonon frequency ($\Delta\omega_{\text{Ge-Ge}}$) of the Ge quantum well with respect to the bulk Ge peak can be determined ($\sim 4.4 \text{ cm}^{-1}$). Using this shift of the Ge quantum well as well as the phonon confinement model, the biaxially compressive strain in the Ge quantum well is estimated to be $\sim 1.25\%$ (Fig. 1(b)).

Si/Ge heterojunction Light Emitting Diode

Fig. 2 shows EL spectra at different temperatures from the Ge quantum well MOS LED with 1 nm Si cap and the device size of $4 \times 10^{-2} \text{ cm}^2$. The drive current is 50 mA at the gate voltage of -8 V. The electron-hole-plasma (EHP) recombination model can be used to fit the EL spectra. The apparent band gap is the low energy edge of the emission peak in the spectra. Device temperatures of 130 K, 210 K, and 320 K are obtained from the fitting of the EL line shapes, while the corresponding temperatures of cold finger in the EL measurement are 10 K, 150 K, and 300 K. The temperature difference is due to the device heating. The apparent energy gap extracted by the EHP model is $\sim 0.52 \text{ eV}$ ($\sim 2.4 \mu\text{m}$), and $\sim 0.56 \text{ eV}$ ($\sim 2.2 \mu\text{m}$) at the temperature of 320 K and 130 K, respectively. Due to the much smaller emission

energy as compared to strained Ge band gap, the 2-2.4 μm light emission is proposed to originate from the type-II Si/Ge heterojunction, i.e., the recombination of electron at Si conduction band and hole at Ge valence band (Fig. 3). To confirm the origin of ~ 0.52 eV emission, the quantum confinement energy of the Si cap and the Ge quantum well are calculated. There are small differences between the theoretic value and the measured data. The possible errors are the surface bending, the Ge phonon (36 meV) emission, and the interdiffusion of Si into Ge quantum well during the Si cap growth. The first two mechanisms reduce the photon emission energy, but the last mechanism increases the photon emission energy. The peak around 1.6 μm is the band edge emission of the Ge quantum wells, and is very weak due to the type II alignment of Si/Ge heterojunction. The Ge wells have a low electron concentration.

The strain enhancement is obtained by the mechanical setup in Fig. 4. The strain level can be obtained from Raman shift and agrees well with the ANSYS simulation and strain gauge measurement [3]. The red shift of EL spectra at 120 K under external tensile strain was found in the Si/Ge heterojunction (Fig. 5), as well as the bulk Si MOS LED (Fig. 6). The red shift of the bulk Si MOS LED is due to the downshift of conduction band and the upshift of the valence band. However, the red shift of the Si/Ge heterojunction MOS LED is smaller than the bulk Si LED (Fig. 7) due to the downshift of both Si conduction band and Ge valence band. The red shift is the difference of these two downshifts. Note the original compressive strain in Ge decreases by the external tensile strain.

Ge on Insulator (GOI) Photodetector

Fig. 8 shows the basic fabrication process of GOI MOS detector including hydrogen ion-implantation and direct wafer bonding techniques. The n-type, (001) germanium substrate was prepared as a “host” wafer. The hydrogen ions with a dose of $1 \times 10^{17} \text{ cm}^{-2}$ and the energy of 200 keV were implanted into the host wafer before bonding to form a deep weakened layer. On the other substrate, 80 nm thermal oxide was grown on the p-type Si substrate to form the “handle” wafer. The handle wafer and host wafer were hydrophilically cleaned in the SC-1 clean and $\text{KOH} : \text{H}_2\text{O}$ solution rinsed in de-ionized water, and initially bonded at the room temperature. The wafer pair were annealed to strengthen the chemical bonds between the interface of the two wafers and to induce layer transfer along the weakened hydrogen-implanted regions by H_2 blistering. The separated surfaces exhibit a root-mean-square roughness of ~ 7 nm after the H_2 blistering. The TEM image of GOI detector is shown in Fig. 9. Fig. 10 shows the typical dark and photo current of a GOI detector under different wavelength exposure. The fiber is pointed to the edge of the gate electrode and the photo-generated carriers can be collected by lateral diffusion/drift. The inset of Fig. 10 is the responsivity of GOI

detector under light exposure. The GOI detector has the responsivity of 270, 200, and 50 mA/W at the wavelength of 850, 1310, and 1550 nm, respectively. The initial speed measurement of GOI detector without GSG RF pad shows 60 % enhancement as compared to bulk Ge detector. The higher speed is expected by using the GSG RF pad on the device. Fig. 11 shows the photo I-V characteristic of GOI MOS detector under external mechanical strain at 300 K. The photocurrent of the GOI and bulk Si detector under external strain enhance $\sim 10\%$ and $\sim 15\%$, respectively as compared to the relaxed devices (The inset of Fig. 11) due to the band gap narrowing from the strain, while the change of dark current is smaller than 2 %. Fig. 12 shows the band diagram of a p-type Si detector under inversion bias. The deep depletion region is formed at inversion bias due to the tunneling of LPD oxide. The photoelectrons are generated in the deep depletion region, and are swept toward the gate electrode. The photoelectrons tunnel from the active layers to the Al gate electrode through the trap-assisted tunneling of LPD oxide. The dark current is mainly determined by the generation rate of minority carrier via interface states at oxide/semiconductor interface. Therefore, the band gap narrowing due to strain has less effect on the dark current as compared to the photo current.

Summary

In summary, the 2 μm Si/Ge heterojunction emission LED, and the high-efficient and high-speed GOI MOS detector are reported for the first time. By the proper design of the strain mechanism, it can possibly further extend the wavelength to mid-infrared for the light emission and enhances the responsivity for detection. The high performance makes it feasible to integrate optoelectronic devices into the Si chip for future applications. Both strain-enhanced light emission and detection from Si/Ge metal-oxide-semiconductor devices are demonstrated.

Acknowledgments

The support of Raman measurement by Prof. Chih-Ta Chia at the National Taiwan Normal University is highly appreciated. This work is supported by National Science Council of ROC under contract Nos. 93-2215-E-002-003 and 93-2215-E-002-017, and US air force (AOARD-04-4072).

References

- (1) C. W. Liu et al., “Light emission and detection by metal oxide silicon tunneling diodes,” *IEDM Tech. Dig.*, pp.749-752, 1999.
- (2) B.-C. Hsu et al., “High Efficient 820 nm MOS Ge Quantum Dot Photodetectors for Short-Reach Integrated Optical Receivers with 1300 and 1550 nm Sensitivity,” *IEDM Tech. Dig.*, pp.91-94, 2002.
- (3) M. H. Liao, M.-J. Chen, T. C. Chen, P.-L. Wang, and C. W. Liu, “Electroluminescence from metal/oxide/strained-Si tunneling diodes,” *Appl. Phys. Lett.*, vol. 86, p. 223502, 2005.
- (4) T. C. Chen, W. Z. Lai, C. Y. Liang, M. J. Chen, L. S. Lee, and C. W. Liu, “Light emission from Al/HfO₂/Silicon diodes,” *Journal of Applied Phys.*, vol. 95, p. 6486, 2004.
- (5) C. W. Liu, S. Maikap, and C.-Y. Yu, “Mobility-Enhancement Technologies,” *IEEE Circuits and Devices Magazine*, p. 21, May/June, 2005.

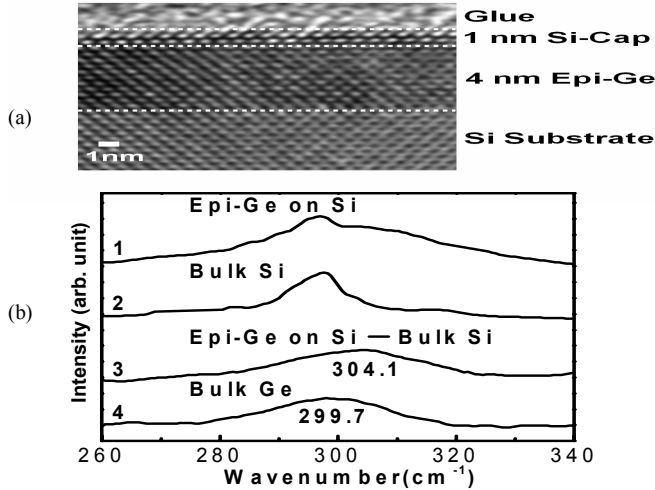


Fig. 1 (a) The cross-sectional transmission electron micrograph of the as-grown Ge quantum well on (100) Si. (b) The Raman spectra of epi-Ge on Si (curve 1), Si substrate (curve 2), pure Ge layer without Si substrate interference (curve 3), and the bulk Ge wafer (curve 4). The blue shift of Ge-Ge peak of curve 3 w.r.t. curve 4 indicates the compressive strain of $\sim 1.25\%$.

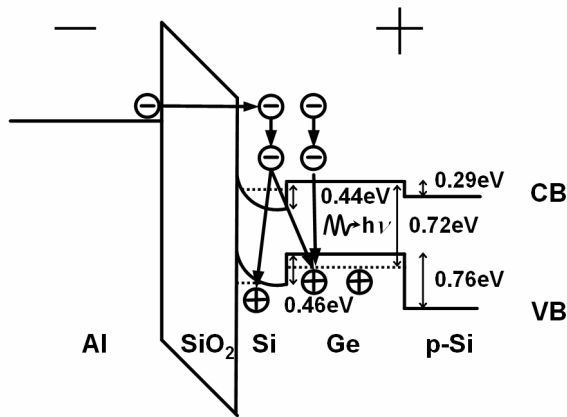


Fig. 3 The schematic band diagram of the strained Ge quantum well (4 nm) device with a Si cap (1 nm) for NMOS tunneling diode. The 2 μm emission is proposed from the transition of the Si conduction band to the Ge valence band.

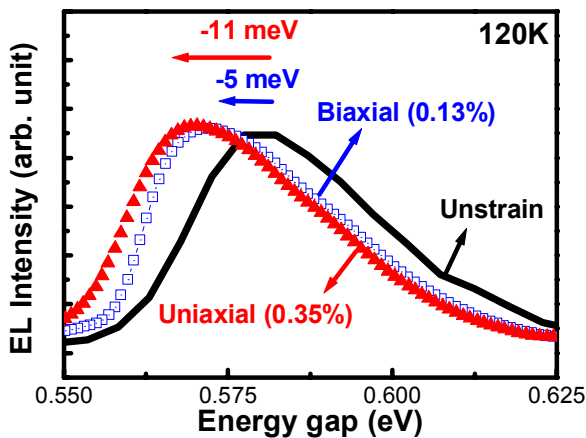


Fig. 5 The EL spectra of a strained Ge/Si heterojunction MOS LED under external 0.13% biaxial tensile strain and 0.35% uniaxial tensile strain at 120K.

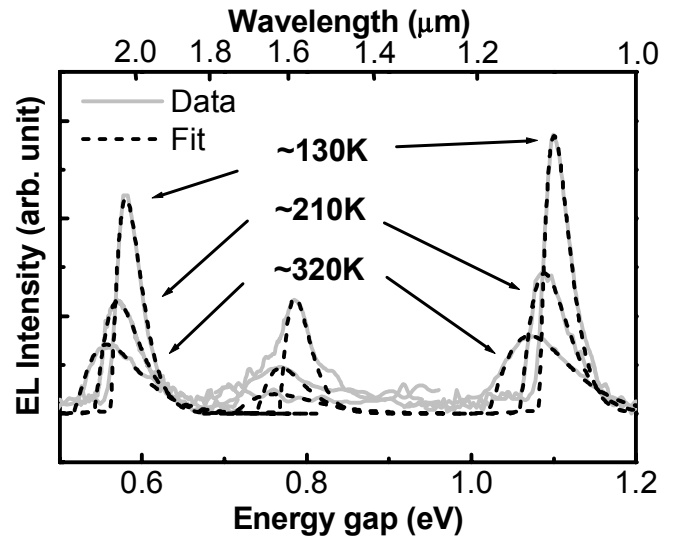


Fig. 2 The electroluminescence spectra of strained Ge/Si heterojunction MOS LED with the fitting curves of the electron-hole plasma recombination model at 130, 210, and 320 K. Three peaks could be corresponding to the Si cap emission, epi-Ge emission, and the Si/Ge heterojunction emission.

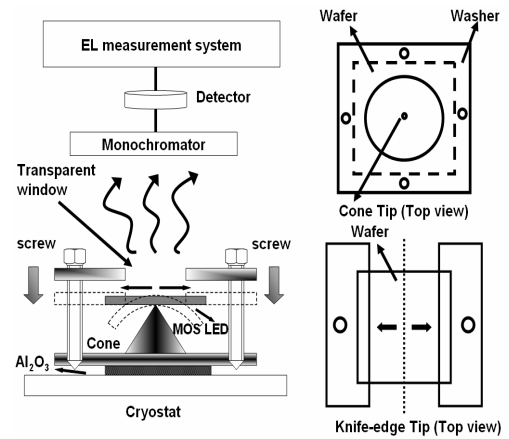


Fig. 4 Schematic diagram of the mechanical setup to apply biaxially and uniaxially mechanical strain in the low temperature cryostat.

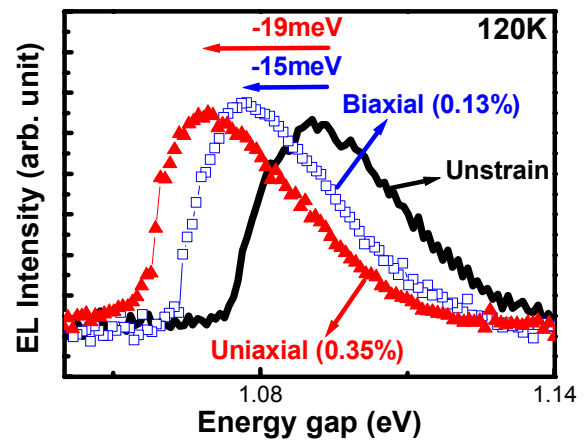


Fig. 6 The EL spectra of a strained Si MOS LED under external 0.13% biaxial tensile strain and 0.35% uniaxial tensile strain at 120K.

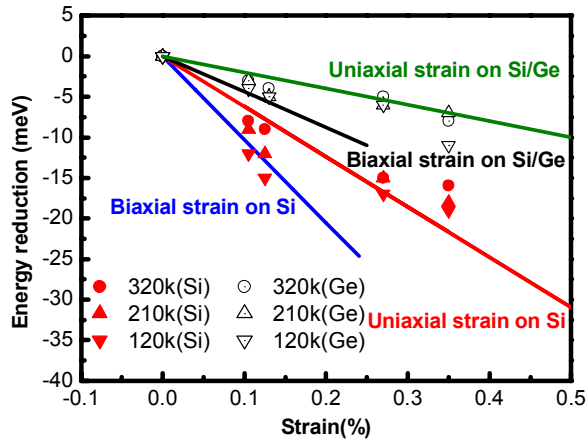


Fig. 7 The theoretical emission energy reduction and the red shift data from EL measurement under external strain. The red shift of strained Ge/Si heterojunction is due to the relative down shift of Si conduction band edge and Ge valence band edge, and is smaller than that of bulk Si.

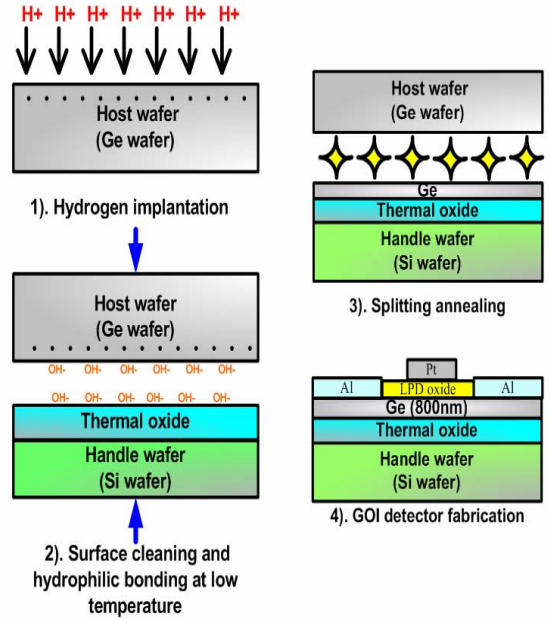


Fig. 8 The fabrication of Ge on insulator (GOI) MOS detector.

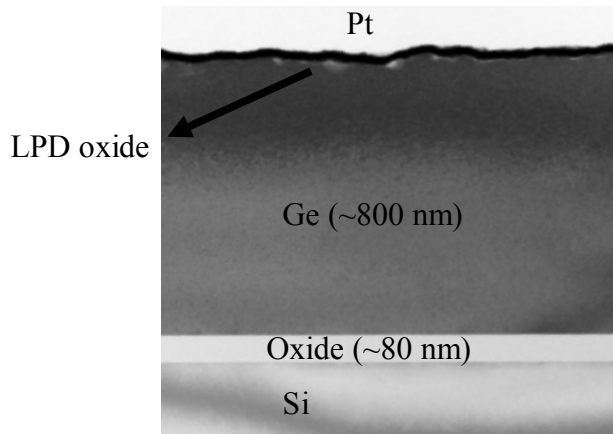


Fig. 9 The cross-sectional transmission electron micrograph of the GOI detector.

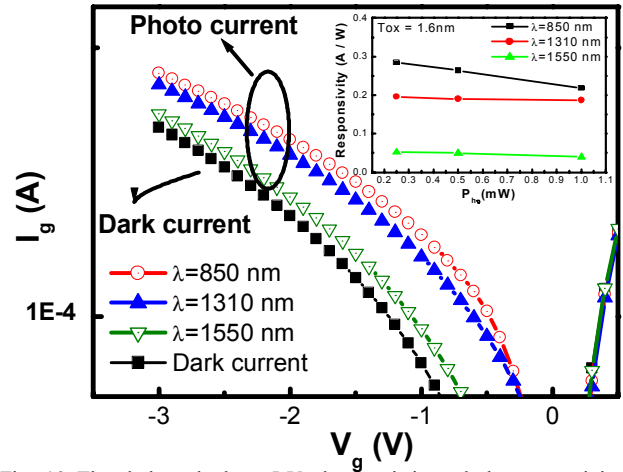


Fig. 10 The dark and photo I-V characteristic and the responsivity vs. different input power of a GOI detector under 850 nm, 1310 nm, and 1550 nm lightwave exposure.

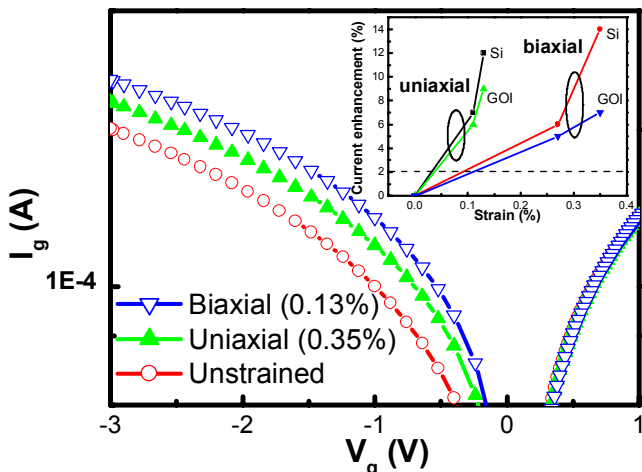


Fig. 11 The photo I-V characteristic (850 nm exposure) of GOI detector under external tensile strain at 300K. The inset of Fig. 11 shows the photo current enhancement of GOI and Si MOS detector vs. mechanical strain. The change of dark current is smaller than 2%.

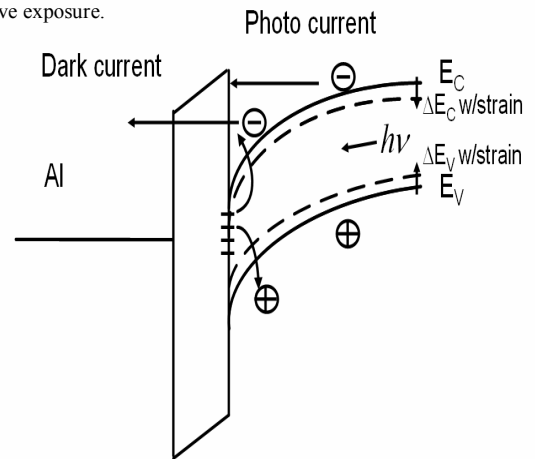


Fig. 12 The band diagram of p-Si photodetector under inversion bias. The photo-generated electrons tunnel through LPD oxide and can be enhanced by band gap narrowing. The dark current is determined by the D_{it} , and hence band gap narrowing due to strain has less effect on dark current.